

## EFFECTS OF THE TIME DELAYS IN AN ENDOREVERSIBLE AND NONENDOREVERSIBLE THERMAL ENGINES WORKING AT DIFFERENT REGIMES

Páez-Hernández R.\*, Portillo-Díaz P.°, Ladino-Luna D.\*

\*Área de Física de Procesos Irreversibles, °Departamento de Ciencias Básicas, Universidad Autónoma Metropolitana-Azcapotzalco, Av. San Pablo No. 180 Col. Reynosa Tamps. CP02200 MÉXICO  
Corresponding Author: phrt@correo.azc.uam.mx

### ABSTRACT

In this work we analyze engine implicit time delays of an endoreversible Curzon-Ahlborn engine using a van der Waals gas working at maximum power regime, we obtain relaxation times, and system phase portrait. When comparing the phase portrait with an endoreversible Curzon-Ahlborn engine using a van de Waals gas working at maximum ecological regime, we observe that eigenvectors have a counter clockwise rotation, as can be seen in the corresponding phase portrait. We find that the total time delay does not destabilize the system steady-state, regardless of this length, and thus it does not seem to play a role in the dynamic-thermodynamic properties trade-off. This result is in accordance with previous studies of endoreversible and non-endoreversible Curzon-Ahlborn engines. Finally we can conclude that it is a fact that the engine dynamic properties are different when the work regimes and working substance change.

### INTRODUCTION

There are many previous works on Finite Time Thermodynamics (FTT), several of them focus on the steady-state energetic properties of the systems. Nevertheless, it is worthwhile to consider the local stability of the system. Santillán et al [1] first studied the local stability of a Curzon-Ahlborn-Novikov (CAN) engine working in a maximum-power-like regime considering the heat resistance and the equal high and low temperature heat transfer coefficients with Newton's heat transfer law. Chimal-Eguia et al. [2] analyzed the local stability of an endoreversible heat engine working in a maximum-power-like regime with Stefan-Boltzman law. Guzman-Vargas et al. [3] studied the effect of heat transfer law and heat transfer coefficients on the local stability of an endoreversible heat engine operating in a maximum-power-like regime. Barranco-Jimenez et al [4] investigated the local stability of a thermo-economic model of a Novikov-Curzon-Ahlborn heat engine. Páez-Hernandez et al. [5] studied the dynamic properties in an endoreversible Curzon-Ahlborn (CA) engine using a Van der Waals gas working substance at maximum power regime. Páez-Hernandez et al. [6] studied the Local stability analysis of a Curzon-Ahlborn engine considering the Van der Waals equation state in the maximum ecological regime. Chimal-Eguia et al. [7] analyzed the local stability of an endoreversible heat engine working in an ecological regime. Páez-Hernández et al [8] studied the dynamic robustness of a non-endoreversible engine working at maximum power output. Sanchez-Salas et al. [9] studied the dynamic robustness of a non-endoreversible engine working in an ecological regime. Huang et al [10] studied the local analysis of an endoreversible heat pump operating at minimum input power for a given heating load with Newton's heat transfer law. Huang [11] analyzed the local asymptotically stability of an irreversible heat pump subject to total thermal conductance constraint. Wu et al [12] studied the

local stability of an endoreversible heat pump with Newton's heat transfer law working at the maximum ecological function.

### TIME DELAYS

In real life situations when the value of a variable is modified, the effect in the dynamic response of the system is not observed immediately. A certain time must elapse until the system begins to respond or "feel" the effect of the changes made. Suppose we modify the concentration of a reactor feed. Our experience and common sense tell us that time passes until the variables that characterize the dynamic behavior of the reactor (e.g. concentration) begin to modify its value relative to their pre-change. These systems are known as dynamical systems. Delayed systems appear naturally in Medicine, Biology and Engineering. These systems have been studied before the last century. Studies in Medicine and Biology begin with Ross' epidemiology models (1911) and others in the early twentieth century, which were studied by Lotka, Volterra and Kostitzin [13]. A distinctive feature of these systems is that their rate of evolution is described by differential equations that include information about the history of the system. The effects of delays are of great interest, since their presence may include complex behavior (oscillations, instability, bad system performance). Páez-Hernández et al [14] studied the effect time delays produced in a mathematical model for the stretch reflex regulatory pathway. Guzmán-Vargas et al [15] studied time-delay effects on dynamics of a two-actor conflict model.

### FIXED POINT AND LINEARIZED SYSTEM WITH DELAYS

Consider a dynamic system which has a single variable with time delays  $\xi$ ,

$$\begin{aligned}\frac{dx}{dt} &= f(x, y_\xi) \\ \frac{dy}{dt} &= g(x_\xi, y)\end{aligned}\quad (1)$$

where subscript  $\xi$  is a time delay variable. Following step by step Strogatz [16] to obtain a linear system,

$$\dot{u} = f(x^* + u, y^* + v_\xi), \dot{v} = g(x^* + u_\xi, y^* + v), \quad (2)$$

where  $u$  and  $v$  represent a small perturbation of the system and  $(x^*, y^*)$  is a fixed point, now we do a Taylor series expansion to Eq. (2) and we consider negligible the terms of two onward, and evaluate the steady-state and we obtain

$$\dot{u} = \left. \frac{\partial f}{\partial x} \right|_{(x^*, y^*)} u + \left. \frac{\partial f}{\partial y_\xi} \right|_{(x^*, y^*)} v_\xi \quad (3)$$

$$\dot{v} = \left. \frac{\partial g}{\partial x_\xi} \right|_{(x^*, y^*)} u_\xi + \left. \frac{\partial g}{\partial y} \right|_{(x^*, y^*)} v. \quad (4)$$

Now we assume that  $u$  and  $v$  are of the form

$$u = A_1 e^{\lambda t} \quad (5)$$

$$u_\xi = A_1 e^{\lambda t} e^{-\lambda \xi} \quad (6)$$

$$v = A_2 e^{\lambda t} \quad (7)$$

$$v_\xi = A_2 e^{\lambda t} e^{-\lambda \xi} \quad (8)$$

where  $\lambda$  is a complex number,  $A_1$  and  $A_2$  are constant.

Substituting (5)-(8) in (3) and (4) leads to the following set of homogeneous linear system for  $A_1$  and  $A_2$ :

$$(f_x - \lambda)A_1 + f_{y_\xi} e^{-\lambda \xi} A_2 = 0 \quad (9)$$

$$f_{x_\xi} e^{-\lambda \xi} A_1 + (g_y - \lambda)A_2 = 0. \quad (10)$$

This system of equations has non-trivial solutions only if the determinant of the matrix of coefficients equals zero, i.e.

$$(f_x - \lambda)(g_y - \lambda) - f_{x_\xi} g_{y_\xi} e^{-2\lambda \xi} = 0. \quad (11)$$

This equation is also called the transcendental characteristic equation, and can be written as

$$H(z) + K(z)e^{-z\xi} = 0, \quad (12)$$

with  $z$  an eigenvalue, and  $H(z)$  and  $K(z)$  are polynomials of second and zero order, respectively.

The solutions to this equation are not obvious because has an infinite number of roots [13]. One way to overcome this situation is to consider the fact a common effect of time delays to destabilize stable fixed points or to stabilize unstable fixed points by sustained oscillations. If we assume that  $(z = i\omega)$ , and substitute in (12), we obtain a complex variable equation.

$$P(\omega) + iQ(\omega) = e^{-i\omega\xi} \quad (13)$$

where  $P(\omega)$  and  $Q(\omega)$  are second and first order polynomials, respectively. We observe that the right hand side of this equation represents the unitary circle whereas the left hand side describes a parabola. The intersection of these two curves could represent a change in the stability of the system. The analysis of intersection between the parabola and the unitary circle leads to the following classification:

- If the parabola does not intersect the unitary circle, and the system is stable to  $\xi = 0$ , then the system is stable and independent of delay.
- If the system is stable for  $\xi = 0$  and the parabola intersects the unit circle, then the system can be affected by delays.

## THE STEADY-STATE CURZON-AHLBORN ENGINE USING A VAN DER WAALS GAS AS WORKING SUBSTANCE

Consider the endoreversible CA heat engine (Figure 1). This engine works between the heat reservoirs  $T_1$  and  $T_2$  ( $T_1 > T_2$ ). The working temperatures at steady state are  $\bar{x}$ , and  $\bar{y}$  ( $T_1 > \bar{x} > \bar{y} > T_2$ ). Heat flows from  $T_1$  to  $\bar{x}$  and from  $\bar{y}$  to  $T_2$  through thermal resistances, with a thermal conductance denoted by  $\alpha$ .

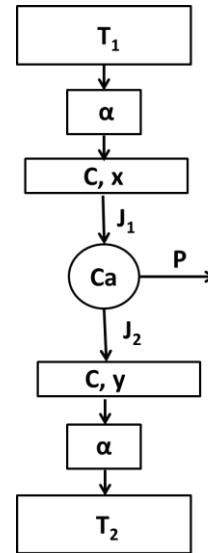


Figure 1: Schematic representation of a CA engine which consists of a Carnot engine (Ca) and the heat reservoirs  $T_1$  and  $T_2$ . The heat exchanges  $J_1$  and  $J_2$  take place through both thermal conductors with the same conductance  $\alpha$ .

Using the endoreversibility hypothesis, an engine working between the reservoir  $\bar{x}$  and  $\bar{y}$  acts like a Carnot engine, although it works in finite time cycles, i.e.

$$\bar{J}_1 = \frac{\bar{x}}{\bar{x} - \bar{y}} \bar{P} \quad (14)$$

and

$$\bar{J}_2 = \frac{\bar{y}}{\bar{x} - \bar{y}} \bar{P} \quad (15)$$

$\bar{J}_1$  and  $\bar{J}_2$  are the steady-state heat flows from  $\bar{x}$  to the engine, and from the engine to  $\bar{y}$  respectively.  $\bar{P}$  is the engine power output.

The CA engine works usually in steady state, so that the heat flux from  $T_1$  to  $\bar{x}$  is  $\bar{J}_1$ , and the heat flux from  $\bar{y}$  to  $T_2$  is  $\bar{J}_2$ ,

$$\bar{J}_1 = \alpha(T_1 - \bar{x}) \quad (16)$$

and

$$\bar{J}_2 = \alpha(\bar{y} - T_2). \quad (17)$$

From equations (14)–(17), and from the definition of efficiency given as,

$$\bar{\eta} = \frac{\bar{P}}{J_1}. \quad (18)$$

it follows that

$$\bar{x} = \frac{T_1}{2} \left(1 + \frac{T_2/T_1}{1-\bar{\eta}}\right) \quad (19)$$

$$\bar{y} = \frac{T_1}{2} (1 - \bar{\eta}) \left(1 + \frac{T_2/T_1}{1-\bar{\eta}}\right). \quad (20)$$

The efficiency of a Curzon-Ahlborn engine working at maximum power output using a van der Waals gas as working substance  $\eta_{vW}$ , was found by Ladino-Luna [17] and it is given as,

$$\eta_{vW} = 1 - \left\{ \sqrt{\tau} + 1/2 (1 - \sqrt{\tau})^2 \lambda_{vW} + \frac{1}{4} (1 - \sqrt{\tau})^2 \left[ \frac{(1-\sqrt{\tau})^2}{2\sqrt{\tau}} - \ln \tau \right] \lambda_{vW}^2 + O(\lambda_{vW}^3) \right\}, \quad (21)$$

with:  $\tau = T_2/T_1$ , and

$$\lambda_{vW} = \frac{1}{\gamma-1} \left( \ln \frac{v_{max}-b}{v_{min}-b} \right)^{-1}, \quad (22)$$

where  $b$  is a constant which depends on the gas,  $\gamma$  is the ratio of the constant-pressure and constant-volume heat capacities  $\gamma = C_p/C_v$ ,  $v_{max}$  and  $v_{min}$  are the subtended volumes maximum and minimum respectively by the gas in a cycle. Now if we consider that  $b$  is smaller than  $v_{max}$  and  $v_{min}$ , table 13.1 [18], then the ratio  $(v_{max} - b)/(v_{min} - b)$  is approximately  $v_{max}/v_{min}$ , this ratio is called volumetric compression ratio  $r_c$ , for Diesel cycle the typical values are 12-15, table 10.1 [19], so we do the calculus using (22) and obtain  $\lambda_{vW} = 1.006$ , which shows that we can use for calculus purposes  $\lambda_{vW} = 1$ , equation (22) gives more values to  $\lambda_{vW}$ , but do not have physical meaning, in accordance with [20].

So we use only the linear approximations of (21), and supposing a value  $\lambda_{vW} = 1$ , and we obtain the approximate expression,

$$\eta_{vW} = 1 - \sqrt{\tau} - \frac{1}{2} (1 - \sqrt{\tau})^2 = \frac{1-\tau}{2} = \frac{\eta_C}{2}. \quad (23)$$

In this approximation we observe a relation between Carnot's efficiency ( $\eta_C$ ) and van der Waals's efficiency ( $\eta_{vW}$ ) at maximum power, which is  $\eta_{vW} = \eta_C/2$ . It is reasonable because  $\eta_{vW}$  is smaller than  $\eta_C$ , so the efficiency of a CA engine working in the maximum power regime using a van der Waals gas working substance is given by (21), with  $\tau = T_2/T_1$ . Now, substituting this efficiency (23), into equations (19) and (20) renders

$$\bar{x} = \frac{T_1 (1+3\tau)}{2 (1+\tau)} \quad (24)$$

and

$$\bar{y} = \frac{T_1}{4} (1 + 3\tau). \quad (25)$$

From (14), and (18)-(20) we can write the power output of the steady- state in terms of  $T_1$  and  $T_2$  ( $T_1$  and  $\tau$ ) and it becomes

$$\bar{P} = \frac{T_1 \alpha (1-\tau)^2}{4 (1+\tau)}. \quad (26)$$

Solving  $T_1$  and  $T_2$ , from equations (19) and (20) results in

$$T_1 = - \frac{2\bar{x}\bar{y}}{\bar{x}-3\bar{y}} \quad (27)$$

and

$$T_2 = \frac{2}{3} \left( 2\bar{y} + \frac{\bar{x}\bar{y}}{\bar{x}-3\bar{y}} \right). \quad (28)$$

Finally substituting (27) and (28) in (26) we obtain the power output in steady-state  $\bar{P}$  as function of  $\bar{x}$  and  $\bar{y}$ ,

$$\bar{P} = - \frac{\alpha(\bar{x}-\bar{y})}{\bar{x}-3\bar{y}}. \quad (29)$$

## LOCAL STABILITY OF AN ENDOREVERSIBLE CURZON-AHLBORN ENGINE

Following Santillán et al [1], a system of differential equations is constructed, which provides information about of the stability engine. Santillán et al. developed a system of coupled differential equations to model the rate of change of intermediate temperature.

Assuming that the temperatures  $x$  and  $y$  correspond to macroscopic objects with heat capacity  $C$ , the differential equations for  $x$  and  $y$  are given by [1]

$$\frac{dx}{dt} = \frac{1}{C} [\alpha(T_1 - x) - J_1] \quad (30)$$

and

$$\frac{dy}{dt} = \frac{1}{C} [J_2 - \alpha(y - T_2)], \quad (31)$$

Both derivatives cancel when  $x, y, J_1$  and  $J_2$  take their steady state values. Under the endoreversibility assumption, the heat flux from  $x$  to the working fluid is  $J_1$  and the heat flux from the Carnot engine to  $y$  is  $J_2$ , so  $J_1$  and  $J_2$  are given in terms of  $x$  and  $y$ , and the power output  $P$  as,

$$J_1 = \frac{x}{x-y} P \quad (32)$$

and

$$J_2 = \frac{y}{x-y} P. \quad (33)$$

It seems reasonable to assume that the power output produced by the CA engine is related to temperature  $x$  and  $y$  in the same way that the power output at steady state  $\bar{P}$  depends on  $\bar{x}$  and  $\bar{y}$  in the maximum power regime (see equation (26)), i.e.,

$$P = \frac{\alpha(x-y)^2}{3y-x}. \quad (34)$$

The substitution (32)-(34) in (30) and (31) leads to the following set of differential equations for temperatures  $x$  and  $y$  of a CA engine performing in maximum-power regime and using a van der Waals gas as working substance.

$$\frac{dx}{dt} = \frac{\alpha[T_1(x-3y)+2xy]}{C(x-3y)} \quad (35)$$

and

$$\frac{dy}{dt} = \frac{\alpha[T_2(x-3y)-2y(x-2y)]}{C(x-3y)}. \quad (36)$$

To analyze the system stability near to the steady state, we proceed by following the steps described in section stability with  $\xi = 0$ . First we define

$$f(x, y) = \frac{\alpha[T_1(x-3y)+2xy]}{C(x-3y)} \quad (37)$$

and

$$g(x, y) = \frac{\alpha[T_2(x-3y)-2y(x-2y)]}{c(x-3y)}. \quad (38)$$

The matrix  $A = \begin{pmatrix} f_x & f_y \\ g_x & g_y \end{pmatrix}$ ,  $A$  is called the jacobian matrix.

Now using Eqs. (37) and (38), we obtain

$$f_x = -\frac{6\alpha(1-\tau)^2}{c(1+3\tau)^2} \quad (39)$$

$$f_y = \frac{8\alpha}{c(1+3\tau)^2} \quad (40)$$

$$g_x = \frac{2\alpha(1+\tau)^2}{c(1+3\tau)^2} \quad (41)$$

$$g_y = -\frac{4\alpha(1+\tau(2+3\tau))}{c(1+3\tau)^2} \quad (42)$$

with  $\tau = T_2/T_1$ .

By substitution of (39)-(42) in Eq. (11) with  $\xi = 0$ , we find that both eigenvalues  $\lambda_1$  and  $\lambda_2$  have real parts, then we can conclude that any perturbation decays exponentially with time and thus that steady-state is stable for every value of  $\alpha$ ,  $C$  and  $\tau = T_2/T_1 > 0$ . The above permit us establish the relaxation times, in [5] was studied the dynamic properties for this engine and is shown that energetic properties of an endoreversible Curzon-Ahlborn engine using a Van der Waals gas working at maximum power output regime (MP) worsens as  $\tau$  decrease to zero, and there is an interval for the Curzon-Ahlborn engine which has efficiency and power output subject to compromise with  $\tau$ , as it has been shown in [1,3,8]. In [6] was studied the dynamic properties for this engine and is shown that energetic properties of an endoreversible Curzon-Ahlborn engine using a van der Waals gas working at maximum ecological regime (ME). This engine has the same characteristic as the maximum power output regime, now our interest is show the behavior for both regimes; in Fig. 2 we compare the relaxation times for both regimes, we observe that relaxation times exhibit approximately the same stability interval.

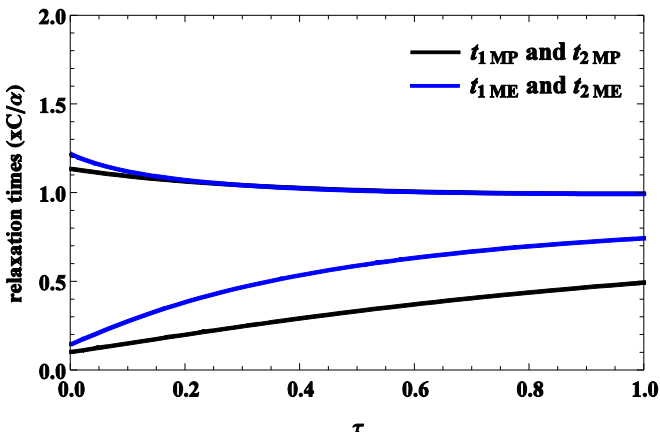


Fig. 2 Plots of relaxation times  $t_1$  and  $t_2$ , in units of  $C/\alpha$ , vs.  $\tau$

However when we compare the portrait phase for both maximum power output and maximum ecological regimes, there is a small difference between the eigenvectors, i.e., there is a rotation for both eigenvectors, this can see in the Fig.3.

## DYNAMIC EFFECTS OF TIME DELAYS

Consider again the systems of delay differential equations given by Eqs. (1) and (2), but now  $\xi = \frac{\pi}{2}$ . They can rewritten as

$$\begin{aligned} \frac{dx}{dt} &= f(x, y_{\pi/2}) \\ \frac{dy}{dt} &= g(x_{\pi/2}, y) \end{aligned}$$

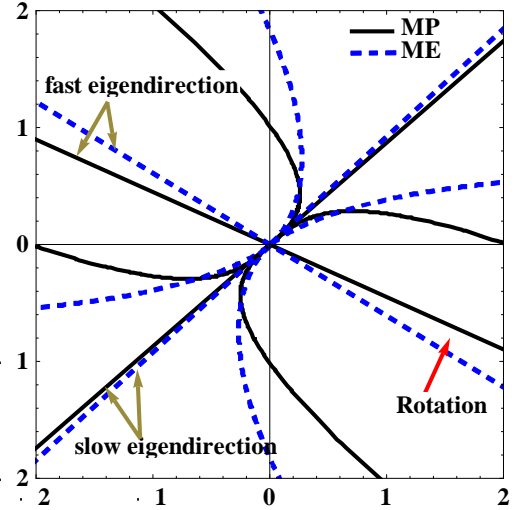


Figure 3. Phase portrait of a Curzon-Ahlborn engine working at two different regimes

with  $f$  and  $g$  as defined in Eqs. (30) and (31). From the fixed points theory with time delays, the time course of small perturbations from the steady state is determined; we can write Eq. (11) as

$$(f_x - \lambda)(g_y - \lambda) - f_y g_x e^{-\lambda\pi} = 0. \quad (43)$$

The stability analysis of a dynamic system involving time delays can be quite complicated due to the fact that, in general, the characteristic equation has an infinite number of solutions. On the other hand, it is known that a common effect of time delays is to destabilize formerly stable steady states by inducing sustained oscillations. To test whether this happens, assume that  $\lambda$  is imaginary ( $\lambda = i\omega$ ) and substitute into the characteristic equation to obtain

$$(-A\omega^2 + B) + iD\omega = e^{(-i\omega\pi)}, \quad (44)$$

with

$$A = \frac{1}{f_y g_x}, \quad B = \frac{f_x g_y}{f_y g_x} \quad \text{and} \quad D = \frac{f_x + g_y}{f_y g_x}.$$

It follows from Eqs. (39)-(42) that  $f_x, g_y < 0$ , while  $f_y, g_x > 0$ . This further implies that constants  $A$ ,  $B$ , and  $D$  are all positive.

The left-hand side of Eq. (44) determines the lower branch of a horizontal parabola in the complex plane. This parabola opens to the left and its vertex is located in the point  $(B, 0)$ . On the other hand, the right-hand side of Eq. (44) determines a unitary circle in the complex plane. The points where these curves cross correspond to values of  $\omega$  and  $\pi$  at which sustained oscillations appear due to a destabilization of the steady state, or vice versa. If both curves never cross, the steady state cannot be destabilized by the total delay  $\pi$ , no matter how long it is. Let  $\rho$  and  $\sigma$  real variables along the real

and the imaginary axes of the complex plane, respectively. In terms of these variables, the equation for the parabola can be written as

$$\rho = B - \frac{A}{D^2} \sigma^2, \quad (45)$$

While the equation for the circle is

$$\rho^2 + \sigma^2 = 1. \quad (46)$$

To find the points where both curves cross, solve for  $\sigma$  in Eq. (45) and substitute into Eq. (46) to obtain

$$\rho^2 - \frac{D^2}{A} \rho + \frac{BD^2 - A}{A} = 0. \quad (47)$$

The solutions to this last equation give the real coordinates of the crossing points. The corresponding imaginary coordinates can then be calculated as  $\sigma = -\sqrt{1 - \rho^2}$ . The solutions of Eq. (47) are

$$\rho_1 = \frac{L}{2} + \frac{1}{2} \sqrt{L^2 - 4K}, \quad (48)$$

$$\rho_2 = \frac{L}{2} - \frac{1}{2} \sqrt{L^2 - 4K}, \quad (49)$$

with  $L = D^2/A$  and  $K = (BD^2 - A)/A$ . From its definition and the fact that  $A$  and  $D$  are positive,  $L$  is also positive and so  $\rho_1 > \rho_2$ . In Fig. 4, the plot of  $\rho_1$ ,  $\rho_2$  and  $\tau$  is shown. Notice that  $\rho_1$  and  $\rho_2$  there are no common points. Therefore, the parabola of Eq. (41) never crosses the unitary circle given by Eq. (45), because  $\rho_1, \rho_2 >$  implies that  $\sigma$  takes imaginary values and the endoreversible Curzon-Ahlborn engine using a Van der Waals gas working at maximum power output regime cannot be destabilized by any time delay. In Fig.4 is shown this result, it is important to remark that there are no common points on both surfaces.

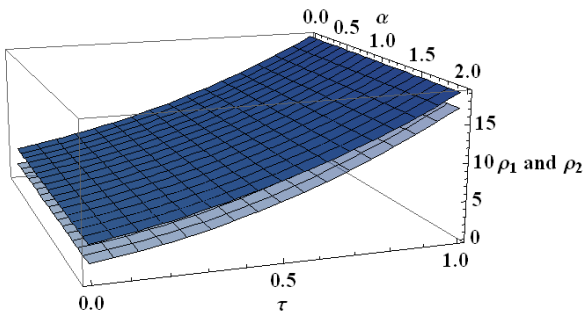


Figure 4. Plot of  $(\rho_1, \rho_2)$ , as given by Eqs. (48) and (49), vs.  $\alpha$  and  $\tau$ , for an endoreversible Curzon-Ahlborn engine using a Van der Waals working at maximum power output regime.

Analogously we can do the same calculus for an endoreversible Curzon-Ahlborn engine using a Van der Waals gas working at maximum ecological regime, and we find a similar behavior and this is shown in Fig. 5.

#### NON-ENDOREVERSIBLE CURZON-AHLBORN ENGINE

Following Páez-Hernández et al. [8], we obtain the relaxation times, the phase portrait diagram and also investigate the effect of delays in time, for reasons of space, here we only show in Fig. 6 the behavior of the effects of delays for a non-endoreversible Curzon-Ahlborn engine using

a Van der Waals gas working at maximum power output regime

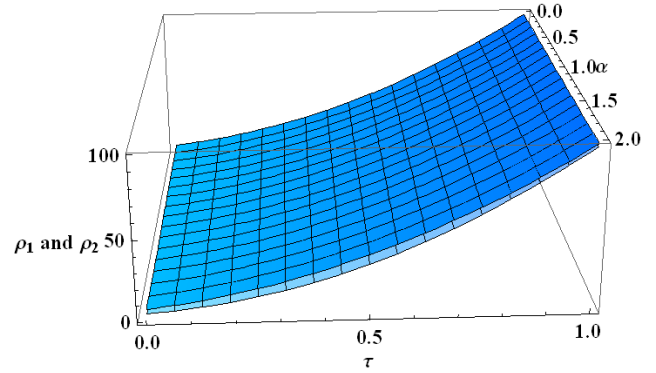


Figure 5. Plot of  $(\rho_1, \rho_2)$ , as given by Eqs. (48) and (49), vs.  $\alpha$  and  $\tau$ , for an endoreversible Curzon-Ahlborn engine using a Van der Waals working at maximum ecological regime.

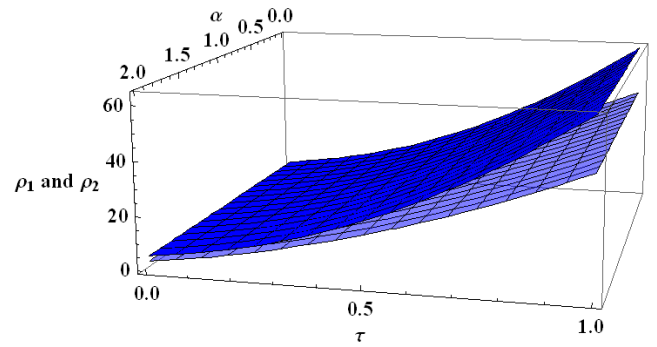


Figure 6. Plot of  $(\rho_1, \rho_2)$ , as given by Eqs. (48) and (49), vs.  $\alpha$  and  $\tau$ , for a non-endoreversible Curzon-Ahlborn engine using a Van der Waals working at maximum power output regime.

#### CONCLUDING REMARKS

In this paper we have extended a previous work by R. Páez-Hernández et al. [5,6] in which the local stability of an endoreversible Curzon-Ahlborn engine working in both maximum power output and maximum ecological regimes. Here, we have considered a Curzon-Ahlborn engine using a Van der Waals gas working at maximum power output regime, also we present the analysis to a non-endoreversible Curzon-Ahlborn in the maximum power regime, taking into account the engine inherent time delays.

Our results indicate that the only effect of different regimes is a rotation in the corresponding eigenvectors in the phase portrait.

Time delays are present in many systems subject to dynamic regulation. In the endoreversible and non-endoreversible Curzon-Ahlborn engine, the inherent time delays are not capable of destabilizing the steady state; thus, they not to play a role in the trade-off between energetic and dynamic properties. This does not have to be true for all energetic-converting systems, though. For instance, time delays are essential to understand the origin of clonus (sustained oscillations in muscle contraction).

#### ACKNOWLEDGMENT

This work was partially supported by CONACYT (SNI). We appreciate the valuable review from F. Miranda Maldonado of the manuscript in English.

## NOMENCLATURE

Symbol	Quantity	SI Unit
$b$	constant which depend on the gas	(m <sup>3</sup> /kg mol)
$C$	Heat capacity	(J/K)
$\bar{P}$	steady-state power output	(W)
$t$	time	(s)
$\bar{x}$	steady-state working hot temperature of the Carnot cycle	(K)
$\bar{y}$	steady-state working cool temperature of the Carnot cycle	(K)
$\alpha$	thermal conductance	(W/K·m)
$\delta x$	small disturbances from the corresponding fixed point values	(m)
$\delta y$	small disturbances from the corresponding fixed point values	(m)
$\lambda_1$	eigenvalue 1	(Hz)
$\lambda_2$	eigenvalue 2	(Hz)
$\xi$	time delays	(s)
$\bar{J}_1$	steady-state heat flow from hot to the engine	(W)
$\bar{J}_2$	steady-state heat flow from the engine to cold	(W)
$t_1$	relaxation time 1	(s)
$t_2$	relaxation time 2	(s)
$T_1$	reservoir at temperature hot	(K)
$T_2$	reservoir at temperature cold	(K)
$\vec{u}_1$	eigenvector corresponding to eigenvalue $\lambda_1$	(m)
$\vec{u}_2$	eigenvector corresponding to eigenvalue $\lambda_2$	(m)
$v_{max}$	maximum subtended volume by the gas in a cycle	(m <sup>3</sup> /kg mol)
$v_{min}$	minimum subtended volumes by the gas in a cycle	(m <sup>3</sup> /kg mol)

## Dimensionless Quantities

$\gamma$	the ratio of the constant-pressure and constant-volume heat capacities
$\bar{\eta}$	steady-state efficiency
$\tau$	ratio of the hot and cold temperatures
$\eta_{vw}$	efficiency of a Curzon-Ahlborn engine working at maximum power output using a van der Waals gas as working substance
$A_1$	arbitrary constant 1
$A_2$	arbitrary constant 2
$B_1$	arbitrary constant 3
$B_2$	arbitrary constant 4
$r_C$	volumetric compression ratio

## REFERENCES

[1] M. Santillán, G. Maya-Aranda and F. Angulo-Brown Local stability analysis of an endoreversible Curzon-Ahlborn engine working in maximum-power-like regime. *J. Phys. D: Appl. Phys.* 34 (13), pp. 2068-2072, 2001.

[2] J.C. Chimal-Eguia, M.A. Barranco-Jimenez and F. Angulo-Brown, Stability analysis of an endoreversible heat engine with Stefan-Boltzmann heat transfer law working in maximum-power-like regime. *Open Syst. Inf. Dyn.*, 13(1), pp. 43-54, 2006.

[3] L. Guzmán-Vargas, I. Reyes-Ramírez and N. Sanchez-Salas, The effect of heat transfer laws and thermal

conductances on the local stability of an endoreversible heat engine. *J. Phys. D: Appl. Phys.* 38(8), pp. 1282-1291, 2005.

[4] M.A. Barranco-Jimenez, R. Páez-Hernández, I. Reyes-Ramírez and L. Guzmán-Vargas, Local stability analysis of a thermo-economic model of a Novikov-Curzon-Ahlborn engine, *Entropy*, 13(9), pp. 1584-1594, 2011.

[5] R. Páez-Hernández, D. Ladino-Luna and P. Portillo-Díaz. Dynamic properties in an endoreversible Curzon-Ahlborn engine using a van der Waals gas as working substance. *Physica A*, 390(20), pp. 3275-3282, 2011.

[6] R. Páez-Hernández, P. Portillo-Díaz, D. Ladino-Luna, M.A. Barranco-Jiménez. Local stability analysis of a Curzon-Ahlborn engine considering the van der Waals equation state in the maximum ecological regime. *ECOS2012. Proceedings of the 25<sup>th</sup> International Conference on Efficiency, Costs, Optimization, Simulation and Environmental Impact of Energy Systems*; June 26-29, Perugia, Italy.

[7] J.C. Chimal-Eguia, I. Reyes-Ramírez and L. Guzmán-Vargas. Local stability of an endoreversible heat engine working in an ecological regime. *Open Syst. Inf. Dyn.*, 14(4), pp. 411-424, 2005.

[8] R. Páez-Hernández, F. Angulo-Brown and M. Santillán. Dynamic Robustness and Thermodynamic Optimization in a Non-endoreversible Curzon-Ahlborn engine. *J. Non-Equilib. Thermodyn.* 31, pp. 173-188, 2006.

[9] N. Sanchez-Salas, J.C. Chimal-Eguia and F. Guzmán-Aguilar. On the dynamic robustness of a non-endoreversible engine working in different operation regimes, *Entropy*, 13(2), pp. 422-436, 2011.

[10] Y.W. Huang, D.X. Sun and Y.M. Kang. Local stability analysis of a class of endoreversible heat pumps. *J. Appl. Phys.* 102(3), pp. 034905, 2007.

[11] Y.W. Huang. Local asymptotic stability of an irreversible heat pumps subject to total thermal conductance constraint. *Energy Convers. Manage.* 50(6). Pp. 1444-1449, 2009.

[12] X. H. Wu, L. G. Chen and F.R. Sun. Local stability of an endoreversible heat pump working at the maximum ecological function, *Chinese J. Eng. Thermophys.* 32(11), pp. 1811-1815 (in Chinese) 2011.

[13] McDonald, N., *Biological Delay Systems: Linear Stability Theory*, Cambridge, UK: Cambridge University Press; 1989.

[14] Ricardo Páez-Hernández and Moisés Santillán, Comparison of the energetic properties and the dynamical stability in a mathematical model of the stretch reflex. *Physica A* 387, pp. 3574-3582, 2008.

[15] A. Rojas-Pacheco, B. Obregón-Quintana, L.S. Liebovitch, L. Guzmán-Vargas. time-delay effects on dynamics of a two-actor conflict model. *Physica A* 392, pp. 458-467, 2013.

[16] H.S. Strogatz. *Non Linear Dynamics and Chaos: With Applications to Physics, Chemistry and Engineering*, Perseus, Cambridge MA, 1994.

[17] D. Ladino-Luna *Rev. Mex. Fis.* 48, pp 575, 2002.

[18] F.F. Huang, *Engineering Thermodynamics an Applications*, 2nd. ed., McMillan Publishing Company. New York, 1989.

[19] J.B. Heywood, *Internal Combustion Engine*, Mc Graw Hill Publishing Company, 1988.

[20] D. Ladino-Luna *J. Energy Institute* 81, (2) 114, 2008.